Dynamics of surface roughening of Cl-terminated Si(100)-(2×1) at 700 K

G. J. Xu, E. Graugnard, V. Petrova, Koji S. Nakayama, and J. H. Weaver
Department of Materials Science and Engineering and Frederick Seitz Materials Research Laboratory, University of Illinois at Urbana-Champaign, Urbana, Illinois 61801

(Received 17 September 2002; revised manuscript received 25 November 2002; published 31 March 2003)

The dynamics of surface roughening and healing induced by Cl on Si(100)-(2×1) were studied with variable-temperature scanning tunneling microscopy. Clean samples were exposed to Cl_2 at room temperature, heated to as high as 700 K, and imaged for periods that exceeded 20 h. Chlorine caused surface roughening via a Cl recycling pathway that created pits and regrowth islands with minimal desorption of $SiCl_2$. This reaction pathway is accessible at ~675 K if the surface is not saturated with Cl. Images showed dimer vacancy creation and pit growth, together with vacancy capture by pits. They also showed dimer vacancy escape from pits and pit annihilation, which had not been reported previously. When the terrace coverage was 0.93 ML, the diffusivity of dimer vacancies along the dimer rows was ~0.7 $Å^2$/sec, about three orders-of-magnitude lower than that on clean Si(100). Single Si adatoms were created on terraces and bonded to Si dimers that were Cl-free. They could form new regrowth dimers or they could be accommodated at the ends of existing islands. Adatoms could also be released from regrowth islands. Pairs of atom vacancy lines separated by one or two Si dimers were observed and the transition between those lines and dimer vacancy lines was recorded. Local areas with (3×2) symmetry were created from the latter. These dynamic changes all require Cl-free Si dimers, and the rate of change of the surface morphology reflects the surface concentration. The rate of change increases with time as the density of bare dimers increases due to the creation of new sites for Cl on an increasingly rough surface and limited desorption.

DOI: 10.1103/PhysRevB.67.125320 PACS number(s): 68.37.Ef, 68.35.Ja, 81.65.Cf

I. INTRODUCTION

Halogens are widely used to modify surfaces during the dry etching of semiconductors. For both fundamental and applied reasons, it is important to develop a more complete understanding of the atomic level processes that give rise to surface patterns. In the last few years, scanning tunneling microscopy (STM) has been used to investigate halogen-induced surface changes, and several studies have focused on Si(100)-(2×1).[1–14] Many of these studies were done at ambient temperature for samples where changes occurred at elevated temperature. In some cases, the initial and final halogen distributions were deduced directly from the STM images to relate etching processes to concentration.[9–11]

Nakayama *et al.*[11] recently studied Cl modification of Si(100)-(2×1) at 775 K. They reported the surprising result that surface roughening occurred at temperatures below the threshold for significant $SiCl_2$ desorption, a process that had gone undetected because of the lack of a desorption product. With STM, they observed dimer vacancies (DVs), dimer vacancy lines (DVLs), pits, and Si regrowth islands (RIs) on the main Si layer. Analysis indicated that the amount of Cl lost was negligible and that areas of regrowth and pit features were nearly the same. To describe roughening without desorption, they proposed a sequence of events in which a Si dimer with two Cl adatoms first undergoes an isomerization reaction, $2SiCl \rightarrow SiCl_2 + Si$. The Si atom with two dangling bonds then escapes onto the terrace. The $SiCl_2$ species can desorb if the temperature is high enough, completing the standard picture of the etching cycle. If desorption is not possible, Nakayama *et al.* proposed that the $SiCl_2$ species could decay by the transfer of its Cl atoms to nearby bare sites and, in this case, the reaction cycle would be completed when the remaining Si atom escaped onto the terrace. The result is a DV, two Si atoms on the terrace, and Cl atoms that can participate in further cycles. In this way, the surface roughens without releasing any telltale desorption species. Since the DVs and Si adatoms are mobile and can also be accommodated at steps, the system would evolve to a dynamic equilibrium configuration where roughening is balanced by healing. These intriguing results led to a host of questions regarding the dynamics associated with surface roughening, the dependence of this reaction pathway on halogen species and concentration, the equilibrium configurations, and the driving force behind roughening.

To investigate the surface dynamics for Cl-Si(100)-(2×1), we undertook studies where it was possible to follow changes in real time with atomic resolution at elevated temperature. The surface concentration was chosen to be high so that the density of all-important Cl-free dimers was low and changes were gradual. Imaging was done in the temperature regime where the rate of desorption of $SiCl_2$ was small. We confirm that the recycling reaction is responsible for the surface roughening and show that this pathway is accessible at ~675 K.

Repetitive imaging at 700 K made it possible to follow the dynamics of individual surface features, revealing processes that had not been observed previously. For example, pit annihilation was observed to occur by DV detachment and escape, and the diffusivity of DVs was reduced to be about three orders-of-magnitude lower than that on clean Si(100), namely, ~0.7 $Å^2$/sec along the dimer row on a terrace with 0.93 ML Cl. RI decay also occurred as Si adatoms detach in the presence of a high Cl concentration. Local areas with DVLs were seen to transform into (3×2) and (5×2) structures that were derived from atomic vacancy

lines. We estimated that the energy barrier that controlled the fluctuations between (3×2) and DVLs was $\sim2.4\pm0.4$ eV. All of these changes require Cl-free Si dimers, and they were quenched when a roughened surface was reexposed to Cl_2 to achieve saturation.

II. EXPERIMENT

The experiments were performed in an ultrahigh vacuum system equipped with a variable-temperature Omicron STM and a sample preparation chamber. The operating pressure was $<4\times10^{-11}$ Torr. The Si wafers were oriented within 0.5° of (100), with a miscut toward [110]. They were *p* type, with B doping and a resistivity of 0.01–0.012 Ω cm. Clean Si(100)-(2×1) surfaces were prepared by degassing at 875 K for ~12 h and heating to 1475 K for 90 sec at pressures lower than 8×10^{-11} Torr.[15] The initial surface defect area was ~0.03 ML.

The Cl_2 source was a solid-state electrochemical cell derived from a AgCl pellet doped with 5% $CdCl_2$. A voltage applied across the cell produced Cl ions that diffused to a Pt mesh electrode and desorbed as Cl_2. The current through the cell controlled the Cl flux, which was kept at 5 μA for these experiments, releasing 1.6×10^{13} molecules per second. Clean Si surfaces were then exposed at room temperature to doses up to 6 mA s to achieve a coverage of 0.99 ML. The initial and final Cl concentrations on the terraces were deduced from the STM images since dimers with Cl are readily distinguished from bare dimers in negative sample bias (-1.3 V) scans at room temperature. At 700 K, the Cl atoms were too mobile to be imaged (diffusion barrier ~0.6 eV). The terrace coverage at a given time during an extended experiment was inferred from the initial and final coverages.

The temperature was monitored with an optical pyrometer during sample preparation and the relationship between temperature and heating power was determined. During scanning, the temperature was adjusted by varying the heating power. Procedurally, it took 40 min for a sample to reach 700 K, and another 1 h to minimize thermal drift. Thereafter, filled-state images were acquired with Pt/Ir tips in a constant current mode with -2.5 V sample bias.

III. RESULTS AND DISCUSSION

A. Surface evolution and Cl recycling

Figures 1(a)–1(c) show the time evolution of Cl-Si(100)-(2×1) through images taken 9.4, 16.8, and 21.1 h after the sample reached 700 K. The initial Cl coverage was 0.99 ML. After 21 h, the sample was quenched to room temperature, and direct counting of bare dimers showed that the final Cl concentration on the terraces was 0.93 ML. Thus, early changes occurred when there were very few Cl-free surface sites but the concentration of Cl-free terrace sites increased with time as the surface roughened and alternate sites for adsorption were created.

In Fig. 1, the dimer rows run diagonally and the scan direction was from left to right. Clearly evident are dark pits elongated along the dimer row direction and bright features representing RIs elongated perpendicular to the dimer rows.

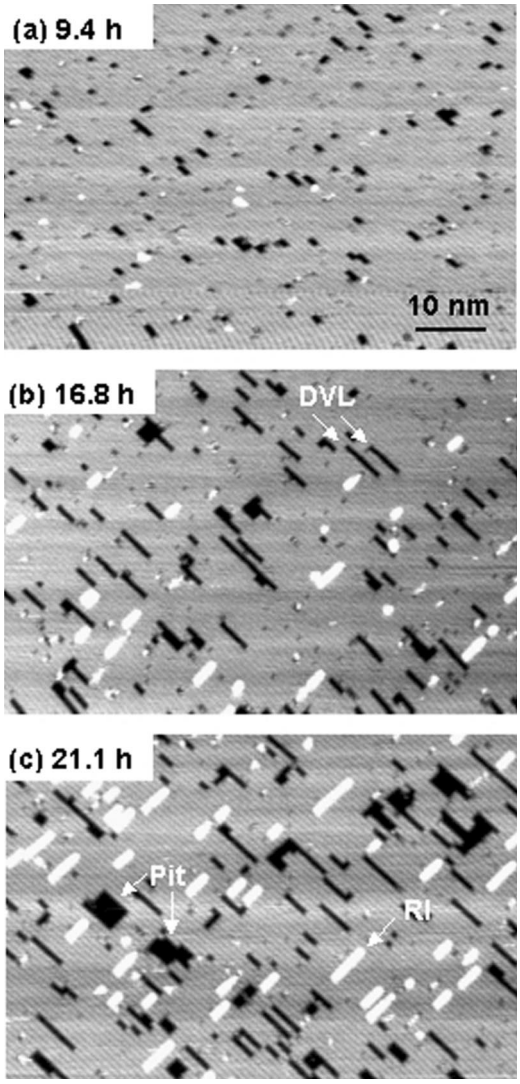

FIG. 1. Time evolution of Cl-Si(100)-(2×1) surface morphology due to Cl recycling reactions that caused pitting and Si atom transfer to the terraces with very slow loss of Cl (as quantified in the text). The images were taken after 9.4 h, 16.8 h, and 21.1 h at 700 K (-2.5 V sample bias). Dimer rows run diagonally, and the scan direction was from left to right. Dark areas are DVLs and pits; the bright features are Si regrowth structures. Small regrowth features and pits in (a) were largely confined to a single dimer row. Pits and RIs were larger in (b) and a few pits extended over several rows because DV diffusion allowed coalescence to occur. The surface imaged in (c) was more dynamic because the terrace concentration had decreased from 0.99 to 0.93 ML and changes could be detected in sequential images. Very few RIs were two rows in width because lateral diffusion was blocked by Cl, and dimer attachment at the sides was kinetically limited. Note that Cl is mobile at 700 K and it is not possible to distinguish bare and Cl-covered dimers. The Cl distribution can be deduced from images at ambient temperature and negative sample bias.

Figure 1(a) shows small pits that were largely confined to single rows after 9.4 h at 700 K (2 to 12 dimer units in length, average 3.5). By 16.8 h, the pits increased in length (2 to 29 dimer units, average 7.7) and a few extended over several rows. Thereafter, the average pit length was at 7.6

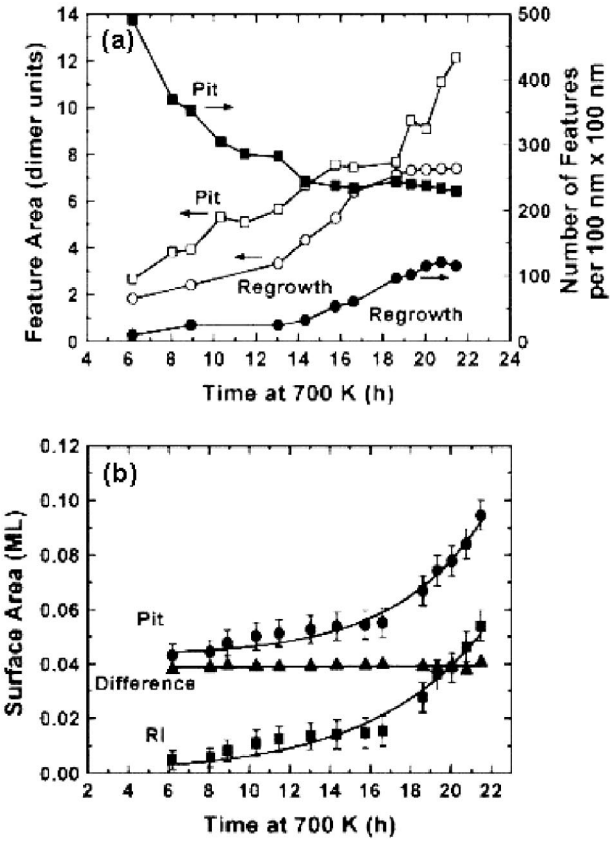

FIG. 2. (a) Average feature area for pits and RIs and the number of features per 100×100 nm^2 area as a function of time at 700 K. While the pits increased slowly in area, they decreased in density due to coalescence. RIs increased in both area and number as the recycling reaction transferred more Si to the terrace and the high concentration of Cl frustrated coalescence. (b) Surface areas of pits and RIs both increased with time at 700 K. The difference between them was nearly constant because pit growth occurred by Si transfer to the terrace. After ~16 h at 700 K, the Cl terrace concentration decreased from 0.99 to ~0.96 ML and the greater density of bare dimers allowed the recycling reaction to accelerate.

dimer units. This suggests that growth was balanced by DV escape (discussed below and in Sec. B). DV escape became increasingly likely as the Cl concentration decreased. The pits in Fig. 1(c) after 21 h were extended laterally because of branching and coalescence across adjacent rows. On the terraces, the RIs grew from 2.2 dimer units at 9.4 h to 7.4 at 16.8 h and their length distribution was then almost constant until at least 21.1 h. Thus, RI extension was ultimately balanced by decay (also discussed in Sec. B), with longer features being more likely to break apart because Si ad-dimers can be lost from the ends or central parts.

Figure 2(a) shows that the average pit area grew from ~3 dimer units at 6 h to ~12 by 21 h, but that the number of pits per 100×100 nm^2 area decreased from ~491 to ~229, confirming that growth involved coalescence. Over that interval, the average RI area grew from ~2 to ~7 dimer units, and the number of RIs per 100×100 nm^2 area increased from ~10 to ~120. Figure 2(b) shows that the surface area of pits and RIs increased gradually with time. Significantly, the difference in pit and RI surface areas on terraces far from steps was constant as pit growth occurred by Si transfer to the terrace. Indeed, the difference, ~0.04 ML, is close to the defect area for the starting surface, ~0.03, suggesting minimal loss of Si over a 21 h period.

Analysis after the sample was cooled showed that the Cl concentration on the terraces had been reduced by 0.06 ML after 21 h at 700 K. About 0.02 ML of this would be due to $SiCl_2$ desorption since there was a 0.01 ML loss of Si. The remainder is likely to have been accommodated at newly created sites on the roughened surface. de Wijs *et al.*[16] considered possible adsorption sites for Cl at single and double DVs, and they showed that these defects could accommodate additional Cl. Since surface roughening provides alternate sites, the density of bare dimers on the terrace increases and, since bare dimers are a necessary condition for the roughening pathway,[11] the system roughens more quickly.

From images like those of Fig. 1, it is clear that few RIs were more than one row wide, even after 21 h at 700 K and despite the fact that numerous single row features were separated by a single dimer unit. Sequential images showed dynamic behavior as RIs grew, shrank, and occasionally joined together lengthwise, but never laterally. The observation of only single-row RIs was surprising since all previous studies of etching and of Si homoepitaxy showed multirow growth that minimized step edge energies.[6,9,17] The present results can be understood in terms of kinetic constraints imposed by the relatively few Cl-free dimers and the barrier for nucleation of a new row at a regrowth structure or an S_A-type step. Mo *et al.*[17] proposed that Si attachment is unstable and that repeated attempts by mobile Si dimers were necessary to form a stable group, and this was confirmed by Pearson *et al.*[18] Row nucleation is possible when diffusion is facile and the concentration of diffusing species is high (as on supersaturated terraces). For our surfaces, Si diffusion requires Cl-free sites. Images collected at room temperature where the distribution could be quantified show that bare sites tend to be concentrated around pits and are less frequent around RIs. Accordingly, we postulate that the dimer lines separating RIs in Fig. 1 are Cl saturated and that those few dimers that do approach a row laterally are rejected before the needed arrival of second and third dimers occurs. For RIs separated by only one or two dimer units, the high Cl concentration would prevent the needed transfer of multiple Si dimers. While RI widening is suppressed, DV accommodation at an existing pit is more facile, even though the barrier for diffusion is likely to be greater than that for a Si atom or dimer, as for the clean surface.[19–25] The tendency of bare dimers to cluster around pits allows DV diffusion. Once captured, the DV contributes to dynamic shape variations at 700 K.

To confirm that the limited lateral extension of RIs is due to the high Cl coverage, we dosed a clean surface with only enough Cl to reach 0.5 ML and then imaged it at 700 K. After 2.5 h, the images showed large pits and large RIs with quasirectangular shapes and low aspect ratios.[26]

B. Dynamics of surface pits and regrowth islands

While the increase in area for pits and RIs is slow under the conditions of Fig. 1, changes in individual features occur

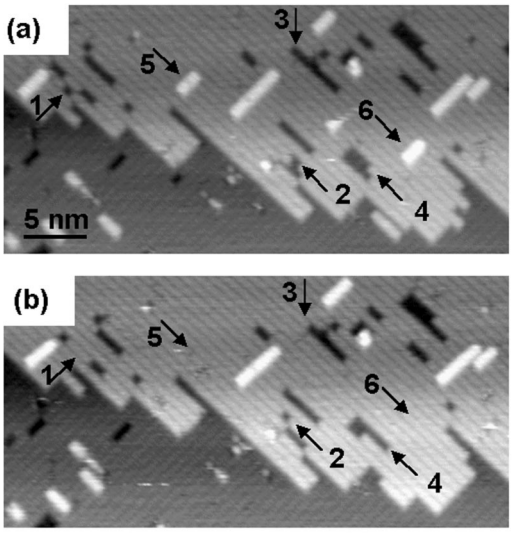

FIG. 3. (a) and (b) Consecutive images showing dynamic surface modification (8.5 min apart after 18.2 h at 700 K, Cl terrace concentration ~0.95 ML, −2.5 V sample bias). Surface processes include (i) pit annihilation, in which pits shrink or disappear, as marked with arrows 1–3; (ii) pit reconstruction without a change in size, as marked with arrow 4; (iii) regrowth island decay, in which RIs shrink or disappear, as marked with arrows 5 and 6.

on a different time scale and can be readily observed in sequential images. This is evident from Figs. 3(a) and 3(b) which were taken 8.5 min apart after 18.2 h at 700 K (terrace concentration ~0.95 ML). They show the creation and diffusion of DVs; the growth, restructuring, and shrinkage of pits; and the equivalent processes for RIs.

Arrows 1–3 in Fig. 3 draw attention to events where pits decreased in size or disappeared. Figure 3(a) shows that pit 1 was derived from two DVs and it was near an S_B-type step. It disappeared in Fig. 3(b) as the DVs were exchanged with two dimers in the adjacent row and were accommodated at the step. Pit 2 crossed two rows but it split as two DVs detached. Pit 3 shrank by 3 units and a 3-unit DVL appeared in the same row ~200 Å away (not shown), where it was blocked by a RI. Pits that were even larger disappeared in consecutive images (not shown). Such local annihilation is achieved through DV detachment and diffusion along the dimer row or, less frequently, across dimer rows. Pit restructuring also occurred without DV gain or loss. Pit 4 was composed of two DVLs that were 8 and 6 dimer units in length. In Fig. 3(b), they rearranged to 3 and 11 units. Statistically, DVLs of odd length greatly outnumbered those of even length.

DV diffusion within a dimer row on clean Si(100)-(2×1) has been attributed by Zhang *et al.*[24] to a wavelike concerted motion which involves four Si atoms: Two fourfold coordinated atoms in the second layer move to the top layer, while two dimerized atoms descend into the second layer. DV diffusion within a dimer row on Cl-Si(100)-(2×1) may follow a similar pathway if there are Cl-free dimers. Concerted motion would require two Si atoms to descend, and this would be unlikely if dangling bonds of top-layer atoms were occupied with Cl atoms.

The DV diffusion evident in Fig. 3 occurred when the Cl terrace concentration was ~0.95 ML.[27,28] If vacancy diffusion does indeed require bare dimers, then diffusion would be negligible on a saturated surface. To test this, we prepared a surface like that of Fig. 1(c) and then reexposed it at room temperature to accumulate 0.995 ML coverage. Subsequent imaging at 700 K showed that the pits, vacancy features, and RIs were nearly frozen. Analysis of an area where there were ~1800 dimer sites, which was imaged after 0.5 h at 700 K, showed only 6 DVs that moved in a 5 min period, consistent with the number of bare dimers.

To quantify DV diffusion, we analyzed results for a terrace with 0.93 ML Cl. At 700 K, we found that the mean-square displacement, $\langle l^2 \rangle$, for single DVs along the dimer rows was ~700 Å^2 in time $t=8.5$ min. Hence the diffusivity, D, was estimated to be ~0.7 Å^2/sec based on $D=\langle l^2 \rangle/2t$. For comparison, the barrier for DV diffusion along the dimer row, E_a, for a clean surface was reported to be 1.4−1.6 eV.[24] If the prefactor γ for the clean surface is 10^{13} sec^{-1},[25] then the diffusivity is $\sim 2.7\times 10^3$ Å^2/sec at $T=700$ K since $D=\gamma \exp(-E_a/\mathrm{kT})a^2$ and $a=3.84$ Å. Therefore, the effect of Cl was to reduce the diffusivity of a DV along the dimer row by about three orders of magnitude compared to clean Si(100). This is reasonable since diffusion would be impeded by the adsorbates.

The decay of RIs is also evident from Figs. 3(a) and 3(b). RIs labeled "5" and "6," both of which were 5 dimer units in length, disappeared after 8.5 min. The bright feature marked with arrows in Fig. 4(a) is probably a Si adatom since its behavior mimics what has been reported for Si adatoms on Si(100).[29,30] It switched sides in Fig. 4(b) and then detached and disappeared in Fig. 4(c). At the same time, the other end of the RI decayed by 4 dimers, probably because there were more bare dimers around the pit. In turn, that pit restructured and broke into two segments.

Swartzentruber[29] deduced that the activation barrier for Si adatom detachment from a RI is ~1.0±0.1 eV for clean Si(100)-(2×1). For Cl-Si(100)-(2×1), the local bonding configuration would be similar is there were available bare dimers and the activation energy might not be too different. In any case, a barrier of 1 eV for detachment can easily be overcome at 700 K.

C. Dynamics of atom vacancy lines and dimer vacancy lines

For Br-Si(100)-(2×1), the coordinated desorption of pairs of $SiBr_2$ units separated by a dimer gives rise to atom vacancy lines (AVLs).[10,31] Such AVLs are also observed for Cl-Si(100) but with less frequency. AVLs can be termed local (3×2) or (5×2) if they are separated by one or two dimer rows. Si atoms within the exposed layer are dimerized.[32,33] Here, we demonstrate that AVLs can transform into DVLs and that the transformation is reversible at 700 K.

Figure 5 shows the dynamic conversion of (3×2) and (5×2) areas (interval 8.5 min). Figure 5(a) shows a (5×2) segment of 11 dimers terminated by a RI and an S_B-type step, as depicted in Fig. 5(b). Five dimers shifted registry in Figs. 5(c) and 5(d) to form short (3×2) and (5×2) regions.

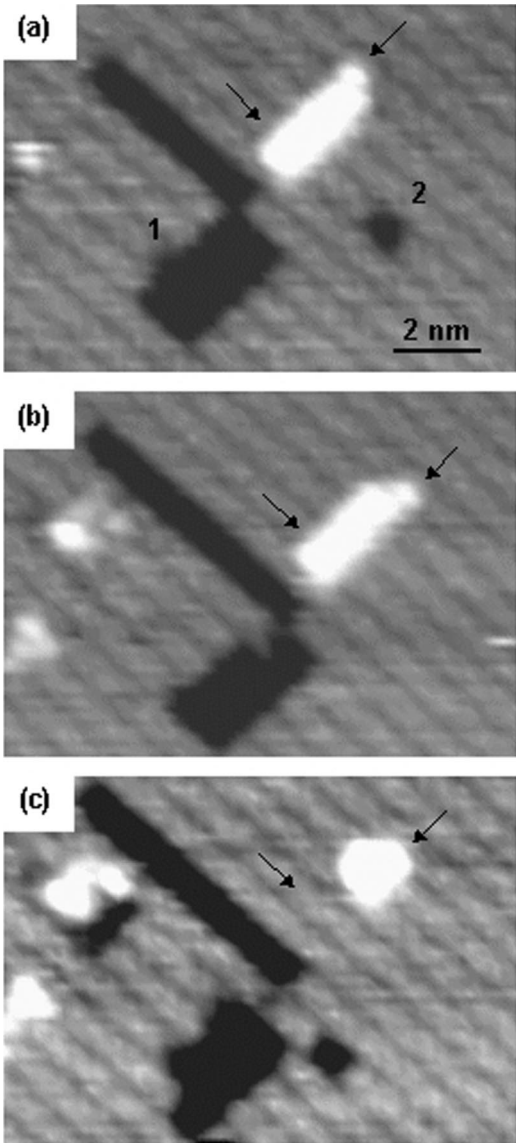

FIG. 4. Decay of a RI shown through consecutive images taken 8.5 min apart after 20 h at 700 K (-2.5 V sample bias). The adatom marked with the arrow in (a) switched to an equivalent site in (b) and disappeared in (c). The other end of the RI lost four dimers. Pit 1 underwent restructuring and ultimately two DVs broke off. Pit 2 diffused out of the image.

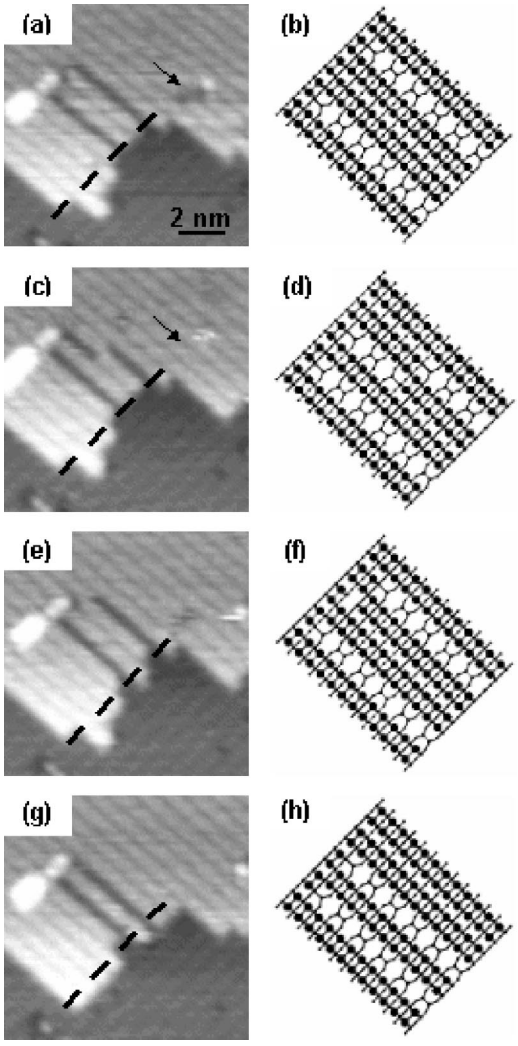

FIG. 5. Dynamics of local (3×2) and (5×2) regions as AVL sections shifted near a step. The images were taken 8.5 min apart after 17.5 h at 700 K (terrace coverage ~0.95 ML, -2.5 V sample bias). A (5×2) segment of 11 dimer units in (a) was terminated by an RI and an S_B-type step. Five dimers shifted registry in (c) to form short regions of (3×2) and (5×2). The arrow points to a pair of DVs that diffused to the step and was accommodated. In (e), the dimers of the (3×2) segment shifted back to their original position. In (g), the (5×2) region converted entirely to a (3×2) region and several dimers changed positions at the step. These configurations are depicted in (b), (d), (f), and (h).

In Figs. 5(e) and 5(f), those dimers shifted back and one row gained 2 dimer units at the step. In Figs. 5(g) and 5(h), the (5×2) region converted entirely to a (3×2) region and there was dimer rearrangement at the step. (To follow the sequence of events, atom by atom, would require faster scanning and a different imaging protocol.) While the step in Fig. 5 could play a role, equivalent conversions also occurred far from steps, provided that they were terminated with a two-row-wide pit. Figures 6(a) and 6(b) reveal a phase transformation as the DVL in Fig. 6(a) transformed to a (3×2) region in Fig. 6(b) terminated with a two-row-wide pit. The equivalent transformation is evident in Figs. 6(c) and 6(d) where a row of dimers shifted to create an AVL.

Figure 7 provides insight into the origin of the (3×2) regions, showing that it is not due to the capture and lining up of mobile single vacancies.[34] The arrows point to a pit derived from DVLs on adjacent rows with 3 units in each, as depicted in Fig. 7(b). The DVL on the right first grew by 2 units, Figs. 7(c) and 7(d). Two dimers then transferred from the left to the right and the left DVL grew by 2 units, Fig. 7(e) and 7(f). Finally, four dimers changed registry by a single atom and created a pair of AVLs of (3×2) local symmetry, Figs. 7(g) and 7(h). Subsequent images showed that Fig. 7(h) converted back to Fig. 7(f) and then Figs. 7(f) converted back to 7(h) as a group of dimers moved in a coordinated fashion.[35] We observe that (3×2) formation occurs only when a DVL is terminated by a two-row-wide pit. The sequence of events in Figs. 5–7 occurred after 15–18 h at

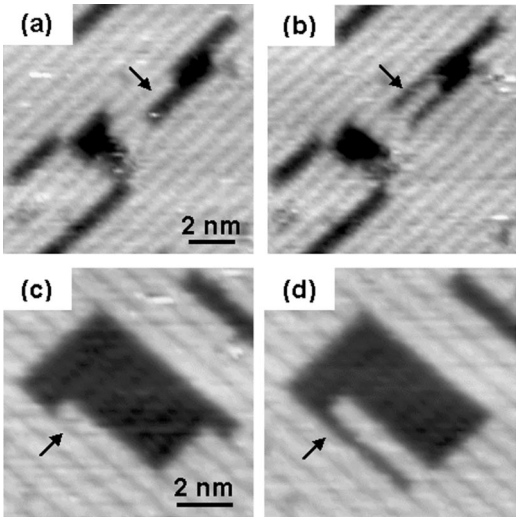

FIG. 6. (a) and (b) show the transformation from a DVL to a (3 $\times$2) of 5 dimer units in length terminated with a two-row-wide pit at one end (images taken 8.5 min apart after 15.5 h at 700 K, terrace coverage $\sim$0.96 ML). (c) and (d) show the equivalent transformation from a DVL to a (3$\times$2) of 10 units in length terminated with a two-row-wide pit at one end (images taken 8.5 min apart after 18 h at 700 K, terrace coverage $\sim$0.95 ML).

700 K when the terrace concentration was $\sim$0.95 ML. There were no (3$\times$2) features after $\sim$10 h because the DVLs were short and limited to a single row.

For clean Si(100), Zhang and Metiu[25] described how a DV can shift across a row (as opposed to diffusion along a row, as discussed above). The first step involved the movement of a Si atom from the adjacent row into the nearest site of the DV. This breaks the dimer bond and costs 2.2 eV. That atom can either return to its starting point or it can move further into the DV and await the arrival of its partner from the original dimer. Rebonding at the new site would regain the 2.2 eV bond energy and the DV will have shifted by 1 unit. We assume that the first step of conversion of a DVL to a pair of AVLs is the same as that for single DV displacement. In particular, the atom identified by the arrow in Fig. 7(f) would move into the vacancy and await its partner. Redimerization would occur in registry or out of registry with the other dimers, shifting it by a full unit or a single atom. If it is the latter, then two AVs are created. Equivalent shifts by other dimers adjacent to the DVL would produce AVLs, as depicted in Fig. 7(h). The process could be started by the jump of a bare Si atom, produced perhaps by an isomerization reaction if the dimer had adsorbed Cl. The attempt frequency for this bare atom can be estimated to be 10^{13} sec^{-1}, following Zhang and Metiu. Experiment indicates that the event probability per unit time was 10^{-4} sec^{-1}, so that the barrier is $\sim 2.4 \pm 0.4$ eV. Finally, experiment shows the conversion from the configuration of Fig. 7(f), or its mirror image, to Fig. 7(h), and statistics indicate that these three configurations are equally probable and thus, energetically equivalent. Note that de Wijs and Selloni[32] considered Cl-terminated Si(100) with (3$\times$2) and (2$\times$1) reconstructions, and they found them to be energetically degenerate. They

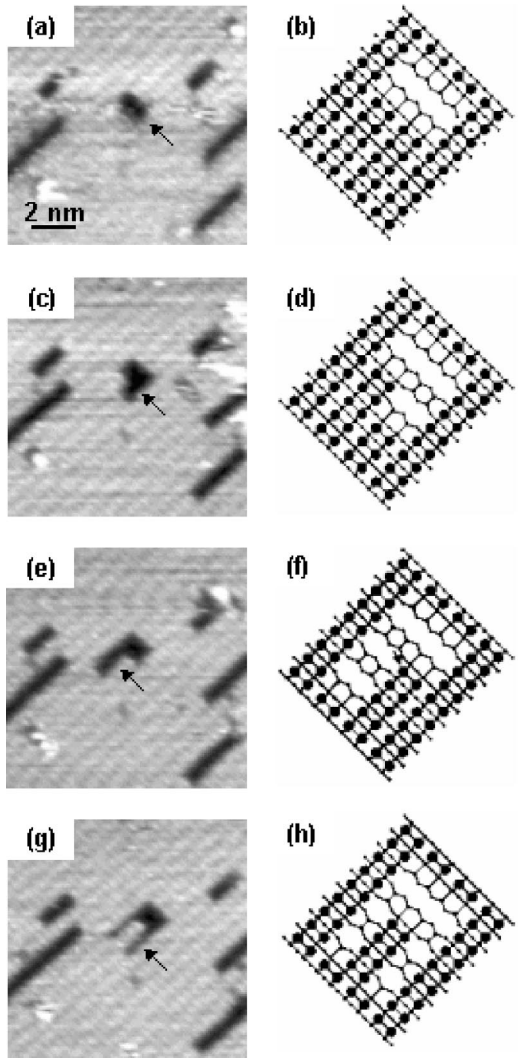

FIG. 7. Formation of a (3$\times$2) segment from a DVL (images taken 8.5 min apart after 16 h at 700 K, -2.5 V sample bias). (a) A pit with two DVLs on adjacent rows. The DVL on the right grew by 2 units in (c) and two dimers transferred from the left to the right in (e) as the left DVL grew by 2 units. Finally, four dimers changed registry by a single atom and created a pair of AVLs that were terminated with a two-row-wide pit. This pathway is depicted in (b), (d), (f), and (h).

also considered Br-terminated Si(100), calculating that the (3$\times$2) configuration was favored by 15 meV/(1$\times$1), in agreement with experiment.[31]

It is likely that the transformation from a DVL to (3$\times$2) starts from the end that is terminated with a two-row-wide pit and then follows an unzipping motion. If the transformation happened in a DVL where both ends were terminated with (2$\times$1) dimers, then the boundary between (3$\times$2) and (2$\times$1) areas would be abrupt and there would be considerable local strain. In this case, the (3$\times$2) would be unstable and it would convert back to (2$\times$1).[36] However, if the transformation happens in a DVL that is terminated with a two-row-wide pit, the strain concentration would be less and the (3$\times$2) would be more stable. The other end of the (3$\times$2) is terminated with (2$\times$1), and that end will be the starting point

for transformation from (3×2) back to (2×1) in a zipping motion. Though the dimers inside the two-row-wide pit could be occupied by Cl, transitions involving (3×2), (5×2), and DVL features require Cl-free second-layer Si in AVLs and DVLs.[37]

IV. CONCLUSIONS

Surface roughening with minimal desorption on Cl-terminated Si(100)-(2×1) has been studied as a function of temperature and coverage. The Cl recycling pathway leads to roughening, and it becomes important at temperatures as low as 675 K. Recycling requires that there be bare dimers. Once the process starts, it produces DVLs that increase the total density of sites for Cl adsorption. This reduces the terrace concentration and accelerates the rate of roughening.

While individual surface features changed dynamically at $\sim$700 K, those changes could be followed when the Cl concentration was high and diffusion was suppressed. Cl-free Si dimers played a critical role in those processes that include pit creation, diffusion, incorporation, and annihilation, as well as regrowth island creation, growth, and decay. AVLs and DVLs transform from one to the other, and the energy between them is $\sim2.4\pm0.4$ eV. The diffusivity of DVs on terraces with a significant Cl concentration was three orders-of-magnitude less than that for clean Si(100). These processes can be frozen by reexposing to Cl to achieve saturation.

While gas phase etching with halogens has been studied for decades, the invention of the STM, and its recent extension to high-temperature imaging, makes it possible to investigate dynamic processes at the nearly atomic level. The parameter space of temperature, surface concentration, and chemical species includes a wide range of phenomena, including those whose existence could not have been predicted.

ACKNOWLEDGMENTS

This work was supported in part by the National Science Foundation and in part by the U. S. Department of Energy, Division of Materials Sciences, under Award No. DEFG02-91ER45439 through the Frederick Seitz Materials Research Laboratory at the University of Illinois at Urbana-Champaign. We thank S. Burdin and E. Sammann of the Center for Microanalysis of Materials for their expert assistance. Stimulating discussions with C.M. Aldao and B.R. Trenhaile are gratefully acknowledged.

[1] J. J. Boland and J. H. Weaver, Phys. Today **51**, 34 (1998).
[2] M. Chander, Y. Z. Li, D. Rioux, and J. H. Weaver, Phys. Rev. Lett. **71**, 4154 (1993).
[3] M. Chander, Y. Z. Li, J. C. Patrin, and J. H. Weaver, Phys. Rev. B **47**, 13 035 (1993).
[4] D. Rioux, M. Chander, Y. Z. Li, and J. H. Weaver, Phys. Rev. B **49**, 11 071 (1994).
[5] D. Rioux, R. J. Pechman, M. Chander, and J. H. Weaver, Phys. Rev. B **50**, 4430 (1994).
[6] M. Chander, D. A. Goetsch, C. M. Aldao, and J. H. Weaver, Phys. Rev. Lett. **74**, 2014 (1995).
[7] D. Rioux, F. Stepniak, R. J. Pechman, and J. H. Weaver, Phys. Rev. B **51**, 10 981 (1995).
[8] M. Chander, D. A. Goetsch, C. M. Aldao, and J. H. Weaver, Phys. Rev. B **52**, 8288 (1995).
[9] K. Nakayama, C. M. Aldao, and J. H. Weaver, Phys. Rev. Lett. **82**, 568 (1999).
[10] K. Nakayama, C. M. Aldao, and J. H. Weaver, Phys. Rev. B **59**, 15 893 (1999).
[11] K. S. Nakayama, E. Graugnard, and J. H. Weaver, Phys. Rev. Lett. **88**, 125508 (2002).
[12] J. J. Boland, Science **262**, 1703 (1993).
[13] C. F. Herrmann and J. J. Boland, Surf. Sci. **460**, 223 (2000).
[14] I. Lyubinetsky, Z. Dohnálek, W. J. Choyke, and J. T. Yates, Jr., Phys. Rev. B **58**, 7950 (1998).
[15] K. Hata, T. Kimura, S. Ozawa, and H. Shigekawa, J. Vac. Sci. Technol. A **18**, 1993 (2000).
[16] G. A. de Wijs, A. De Vita, and A. Selloni, Phys. Rev. B **57**, 10 021 (1998).
[17] Y.-W. Mo, B. S. Swartzentruber, R. Kariotis, M. B. Webb, and M. G. Lagally, Phys. Rev. Lett. **63**, 2393 (1989).
[18] C. Pearson, M. Krueger, and E. Ganz, Phys. Rev. Lett. **76**, 2306 (1996).
[19] The energy barriers for ad-dimer diffusion along and across dimer rows are 1.09 ± 0.05 eV and 1.36 ± 0.06 eV, respectively (see Refs. 20 and 21). For adatom diffusion, they are 0.67 ± 0.08 eV and ~1.0 eV (Refs. 22 and 23). For DV diffusion, they are 1.4–1.6 eV and >2 eV (Refs. 24 and 25).
[20] B. Borovsky, M. Krueger, and E. Ganz, Phys. Rev. Lett. **78**, 4229 (1997).
[21] B. Borovsky, K. Krueger, and E. Ganz, Phys. Rev. B **59**, 1598 (1999).
[22] Y. Mo, J. Kleiner, M. B. Webb, and M. G. Lagally, Phys. Rev. Lett. **66**, 1998 (1991).
[23] Y. Mo, J. Kleiner, M. B. Webb, and M. G. Lagally, Surf. Sci. **268**, 275 (1992).
[24] Z. Zhang, H. Chen, B. Bolding, and M. Lagally, Phys. Rev. Lett. **71**, 3677 (1993).
[25] Z. Zhang and H. Metiu, Phys. Rev. B **48**, 8166 (1993).
[26] G. J. Xu, K. S. Nakayama, B. R. Trenhaile, C. M. Aldao, and J. H. Weaver, following paper, Phys. Rev. B **67**, 125321 (2003).
[27] Images obtained for new areas and for small areas that were scanned dozens of times to follow reaction, image by image, gave no evidence of tip-induced changes for negative sample bias. See, however, Ref. 28 for tunneling-electron-induced Br hopping for positive bias above 0.8 V.
[28] K. S. Nakayama, E. Graugnard, and J. H. Weaver, Phys. Rev. Lett. **89**, 266106 (2002).
[29] B. Swartzentruber, Phys. Rev. B **55**, 1322 (1997).
[30] B. S. Swartzentruber (private communication).
[31] E. Graugnard, K. S. Nakayama, and J. H. Weaver (unpublished).
[32] G. A. de Wijs and A. Selloni, Phys. Rev. B **64**, 041402 (2001).

[33] Line profiles along AVLs showed that the distance between adjacent valleys or peaks was ~7.7 Å. The positions of valleys or peaks in a line profile in a filled-state image were offset by ~3.8 Å compared to those in an empty-state image.

[34] C. F. Herrmann and J. J. Boland, Phys. Rev. Lett. **87**, 115503 (2001).

[35] Changes from (3×2) to (5×2) have also been observed, but this is a rare event.

[36] The (3×2) structure has never been observed for a clean Si(100) surface because these out-of-phase dimer rows are energetically unfavorable due to back bond stress.

[37] C. F. Herrmann, D. Chen, and J. J. Boland, Phys. Rev. Lett. **89**, 096102 (2002), reported that second-layer Si dimers in AVLs were Cl terminated. This would be surprising since Cl should impede the dynamic conversion between AVLs and DVLs. To confirm this we reexposed the sample to chlorine to saturate the surface. This quenched any further conversion.